Determination of Dihedral Angles in Peptides through Experimental and Theoretical Studies of α-Carbon Chemical Shielding Tensors

J. Heller,[†] D. D. Laws,[‡] M. Tomaselli,[‡] D. S. King,[§] D. E. Wemmer,[‡,⊥] A. Pines,*[,‡,||] R. H. Havlin,[£] and E. Oldfield[£]

Contribution from the Graduate Group in Biophysics, Department of Chemistry, and Howard Hughes Medical Institute, Department of Molecular and Cell Biology, University of California, Berkeley, California 94720, Structural Biology Division and Materials Sciences Division, Lawrence Berkeley National Laboratory, Berkeley, California 94720, and Department of Chemistry, University of Illinois at Urbana−Champaign, Urbana, Illinois 61801

Received January 15, 1997. Revised Manuscript Received June 10, 1997[⊗]

Abstract: A simple method for the determination of backbone dihedral angles in peptides and proteins is presented. The chemical-shift anisotropies (CSA) of the central alanine α-carbon in powdered crystalline tripeptides, whose structures have been determined previously by X-ray crystallography, were measured by cross-polarization magic-angle-spinning nuclear magnetic resonance. The experimental CSA values were correlated with *ab initio* chemical-shielding calculations over Ramanchandran φ/ψ space on an *N*-formyl-L-alanine amide fragment. Using this correlation, φ/ψ probability surfaces for one of the tripeptides were calculated based only on the α-carbon CSA, allowing a prediction of backbone angles. Dihedral angles predicted by these calculations fall within ±12° of the values determined by crystallography. This approach should be useful in the determination of solid-state protein structure.

Introduction

Since the early 1980s, the development of nuclear magnetic resonance (NMR) as a tool for biological structure determination has given rise to a large number of isotopic labeling schemes and pulse sequences for the study of proteins in solution. Because these techniques depend on the fast tumbling of molecules in solution, they are not applicable to large molecules and complexes or to systems which exist naturally in ordered or partially-ordered states, for example, solids, membranes, and other aggregates. Indeed few physical techniques exist for the determination of detailed structures in large solid-state systems lacking long-range order. Solid-state NMR (SSNMR), however, is now developing into an important tool for such studies. Recently, structural studies of peptides and proteins that aggregate, such as those responsible for Alzheimer's disease[1] and prion diseases,[2] of membrane proteins such as bacteriorhodopsin[3,4] and glycophorin A,[5] and of large systems which do not fall into the fast-tumbling regime[6,7] have been carried out via SSNMR. Although many SSNMR techniques have been developed recently to measure both distances[8−11] and dihedral angles[12−15] in solids, less information is available from these methods than from a solution-state experiment because of limitations on isotopic labeling and resolution.

One possible means for augmenting the information from SSNMR is to use *ab initio* chemical-shielding computations to gain insight into the backbone structure of a protein. In such methods, the chemical shielding is calculated as a function of the backbone (and potentially the side chain) torsion angles. Correlations between isotropic chemical shifts and secondary structure in proteins have been observed in both liquids[16,17] and solids[2,18,19] and have been reproduced in theoretical calculations.[20,21] Such correlations allow the determination of chemi-

* Alexander Pines, MSD, Lawrence Berkeley Laboratory, 1 Cyclotron Road, Berkeley, CA 94720. phone: (510) 642 1220. fax: (510) 486 5744. e-mail: pines@cchem.berkeley.edu.

[†] Graduate Group in Biophysics, University of California, Berkeley.

[‡] Department of Chemistry, University of California, Berkeley.

[§] Howard Hughes Medical Institute, University of California, Berkeley.

[⊥] Structural Biology Division, Lawrence Berkeley National Laboratory.

[||] Materials Sciences Division, Lawrence Berkeley National Laboratory.

[£] University of Illinois at Urbana−Champaign.

[⊗] Abstract published in *Advance ACS Abstracts,* August 1, 1997.

(1) Lansbury, P. T. J.; Costa, P. R.; Griffiths, J. M.; Simon, E. J.; Auger, M.; Halverson, K. J.; Kocisko, D. A.; Hendsch, Z. S.; Ashburn, T. T.; Spencer, R. G. S.; Tidor, B.; Griffin, R. G. *Nature Struct. Biol.* **1995**, *2*, 990−998.

(2) Heller, J.; Kolbert, A. C.; Larsen, R.; Ernst, M.; Bekker, T.; Baldwin, M.; Prusiner, S. B.; Pines, A.; Wemmer, D. E. *Protein Science* **1996**, *5*, 1655−1661.

(3) Creuzet, F.; McDermott, A.; Gebhard, R.; van der Hoef, K.; Spijker-Assink, B.; Herzfeld, J.; Lugtenburg, J.; Levitt, M. H.; Griffin, R. G. *Science* **1991**, *251*, 783−786.

(4) Griffiths, J. M.; Lakshmi, K. V.; Bennett, A. E.; Raap, J.; VanDer Wielen, C. M.; Lugtenburg, J.; Herzfeld, J.; Griffin, R. G. *J. Am. Chem. Soc.* **1994**, *116*, 10178−10181.

(5) Smith, S. O.; Jonas, R.; Braiman, M.; Bormann, B. J. *Biochemistry* **1994**, *33*, 6334−6341.

(6) Christensen, A. M.; Shaefer, J. *Biochemistry* **1993**, *32*, 2868−2873.

(7) Williams, J. C.; McDermott, A. E. *Biochemistry* **1995**, *34*, 8309−8319.

(8) Raleigh, D. P.; Levitt, M. H.; Griffin, R. G. *Chem. Phys. Lett.* **1988**, *146*, 71−76.

(9) Gullion, T.; Schaefer, J. *J. Magn. Reson.* **1989**, *81*, 196−200.

(10) Tycko, R.; Dabbagh, G. *Chem. Phys. Lett.* **1990**, *173*, 461−465.

(11) Ishii, Y.; Terao, T. *J. Magn. Res., Series A* **1995**, *115*, 116−118.

(12) Schmidt-Rohr, K. *Macromolecules* **1996**, *29*, 3975−3981.

(13) Feng, X.; Lee, Y. K.; Sandstrom, D.; Eden, M.; Maisel, H.; Sebald, A.; Levitt, M. H. *Chem. Phys. Lett.* **1996**, *257*, 314−320.

(14) Tycko, R. At the *Experimental NMR Conference*; Asilomar, California, 1996.

(15) Mehta, M.; Bower, P.; Gregory, D.; Zebroski, H.; Drobny, G. At the *Experimental NMR Conference*; Asilomar, CA, 1996.

(16) Spera, S.; Bax, A. *J. Am. Chem. Soc.* **1991**, *113*, 5490−5492.

(17) Wishart, D. S.; Sykes, B. D. *J. Biomolecular NMR* **1994**, *4*, 171−180.

(18) Saito, H. *Magn. Reson. in Chemistry* **1986**, *24*, 835−852.

(19) Saito, H.; Ando, I. *Annu. Rep. NMR Spectrosc.* **1989**, *21*, 209−290.

(20) de Dios, A. C.; Pearson, J. G.; Oldfield, E. *Science* **1993**, *260*, 1491−1496.

S0002-7863(97)00124-8 CCC: $14.00

cal-shift/shielding surfaces[16,22−24] as a function of the dihedral angles. Coupling these calculations with experimental chemical-shift data has permitted both the further refinement of solution structures,[25−27] as well as probability-based predictions of dihedral angles.[28]

In this paper, we introduce a technique for the determination of backbone dihedral angles in solid-state peptides and proteins which exploits the additional information contained in the chemical-shift anisotropy through the measurement of the chemical-shift tensor and comparison with theoretical calculations via the Z-surface method.[28] Whereas previously two or three experimental isotropic chemical shifts would be needed to determine a unique (ϕ/ψ) pair,[28] this can now be achieved in solids by using just the three components of the chemical-shift anisotropy (CSA) of a single α-carbon (C_α). This technique is experimentally simple: using a 1-D cross-polarization magic-angle-spinning[29,30] spectrum at spinning speeds slow compared to the CSA (slow CPMAS), one can derive the CSA for a singly ^{13}C labeled sample. If a 2-D CPMAS experiment[31−40] is used to resolve any overlap in the many spinning sidebands, this method should also be applicable to samples with multiple ^{13}C labels.

We have measured the $^{13}C_\alpha$ CSA of the central alanine in three crystal forms of the tripeptides glycyl-L-alanyl-L-valine[41] (G*AV) and L-alanyl-L-alanyl-L-alanine[42,43] (A*AA and A*AA-hemihydrate) by slow CPMAS experiments. The measured values correlate well with those calculated by *ab initio* methods using ϕ and ψ angles around the central alanine C_α taken from the known crystal structures. Using the correlation for the A*AA and A*AA-hemihydrate peptides and the measured CSA of G*AV, we calculated ϕ/ψ space probability surfaces (Z-surfaces) for the alanine C_α in G*AV. The highest calculated probability is within ±12° in both ϕ and ψ of the values determined in the X-ray crystal structure. Although in this work we determine only the correlation for alanine residues and for backbone dihedral angles, the method is general and can be extended to other amino acids and possibly to side-chain dihedral angles with the addition of more tensor restraints.

Experimental Section

Fmoc-^{13}C Amino Acids. $^{13}C_\alpha$-labeled alanine (Cambridge Isotope Laboratories, Andover, MA) was Fmoc-protected in a manner similar to one previously described.[44] To 3.75 mmol of alanine dissolved in H_2O (60 mL), 0.945 g (11.25 mmol) of sodium bicarbonate ($NaHCO_3$) was added. After dissolving 1.265 g (3.75 mmol) of *N*-(9-fluorenylmethoxycarbonyloxy) succinimide (Fmoc-*O*-Suc) in acetone (60 mL), the mixtures were combined. The cloudy mixture became clear after stirring for 24 h, at which point the acetone was removed by rotary evaporation. Citric acid (1 M) was used to precipitate Fmoc-$^{13}C_\alpha$-alanine from the aqueous solution. Ethyl acetate (EtOAc) (150 mL) was added to redissolve the precipitate. The mixture was transferred to a separatory funnel, and the layers were separated. The aqueous layer was washed with EtOAc (100 mL). The combined organic layers were then washed with H_2O (2 × 100 mL) and saturated NaCl (2 × 100 mL). The organic layers were dried over magnesium sulfate, and the solvent was removed by rotary evaporation. The product was used for solid-phase peptide synthesis without further purification.

Tripeptides. G*AV and A*AA were synthesized using N-Fmoc protected amino acids on an Applied Biosystems 431A peptide synthesizer. The peptides were cleaved from the resin and deprotected by stirring for 3 h in a 95% (v/v) trifluoroacetic acid (TFA)/H_2O solution. The mixture was filtered to remove resin. TFA was removed by rotary evaporation, followed by lyophilization. The cleaved A*AA was then redissolved in H_2O and purified by reversed-phase HPLC on a Vydac C-18 column. Purity and identity of all samples were checked by electrospray-ionization mass spectrometry (Hewlett-Packard 5989A).

Crystallization. Peptides were crystallized following the protocols described previously, with slight modifications made in order to crystallize larger quantities. In all cases, small crystal clusters were obtained; large single crystals are not necessary in this approach. G*AV[41] was dissolved in a minimal volume of warm H_2O, and the solution was placed in a Petri dish. The dish was then placed into a sealed container over a reservoir of methanol. Due to vapor diffusion, small crystals formed quickly, and crystallization was complete within a day. A*AA was crystallized in two crystal forms.[42,43] The first, A*AA-hemihydrate (needles), was formed by dissolving the tripeptide in a solution of 20% *N*,*N*′-dimethylformamide (DMF)/H_2O and placing the solution in a glass Petri dish. The solvent was allowed to evaporate slowly. The second crystal form of A*AA (plates) was formed by a similar procedure, except that the initial concentration of DMF was 60%.

The dihedral angles around the central alanine for the peptides as determined by the crystal structures were as follows:[41−43] G*AV: $\phi = -68.7°$, $\psi = -38.1°$; A*AA molecule A: $\phi = -143.4°$, $\psi = 160.2°$ and A*AA molecule B: $\phi = -164.1°$, $\psi = -149.0°$; A*AA-hemihydrate molecule A: $\phi = -145.7°$, $\psi = 145.5°$ and A*AA-hemihydrate molecule B: $\phi = -156.2°$, $\psi = 149.9°$.

Solid-State NMR. All ^{13}C NMR spectra were obtained at 7.07 Tesla (corresponding to a ^{13}C Larmor frequency of 75.74 MHz) on a home-built spectrometer based on a Tecmag (Houston, Texas) pulse programmer. A Chemagnetics (Fort Collins, CO) 4-mm double-resonance MAS probe was used for all experiments. Spinning speeds were controlled to ±1 Hz using a home-built spinning-speed controller. CP contact time was 2.5 ms, the ^1H decoupling field strength was 108 kHz, and the recycle delay was 1.5 s. For each crystal form studied, slow CPMAS experiments at three spinning speeds were carried out.

The experimental data was fit by integrating a simulation program into a nonlinear least-square optimization routine. Four-parameters,

(21) Laws, D. D.; de Dios, A. C.; Oldfield, E. *J. Biomol. NMR* **1993**, *3*, 607−612.
(22) de Dios, A. C.; Oldfield, E. *J. Am. Chem. Soc.* **1994**, *116*, 5307−5314.
(23) Laws, D. D.; Le, H.; de Dios, A. C.; Havlin, R. H.; Oldfield, E. *J. Am. Chem. Soc.* **1995**, *117*, 9542−9546.
(24) Asakawa, N.; Hiromichi, K.; Ando, I. *J. Mol. Structure* **1994**, *323*, 279−285.
(25) Kuszewski, J.; Qin, J.; Gronenborn, A. M.; Clore, G. M. *J. Magn. Reson. B* **1995**, *106*, 92−96.
(26) Pearson, J. G.; Wang, J. F.; Markley, J. L.; Le, H.; Oldfield, E. *J. Am. Chem. Soc.* **1995**, *117*, 8823−8829.
(27) Luginbühl, P.; Szyperski, T.; Wüthrich, K. *J. Mag. Res. B* **1995**, *109*, 229−233.
(28) Le, H.; Pearson, J. G.; de Dios, A. C.; Oldfield, E. *J. Am. Chem. Soc.* **1995**, *117*, 3800−3807.
(29) Pines, A.; Gibby, M. G.; Waugh, J. S. *J. Chem. Phys.* **1973**, *59*, 569−590.
(30) Schaefer, J.; Stejskal, E. O. *J. Am. Chem. Soc.* **1976**, *98*, 1031−1032.
(31) Bax, A.; Szeverenyi, N. M.; Maciel, G. E. *J. Magn. Reson.* **1983**, *52*, 147−152.
(32) Gan, Z. *J. Am. Chem. Soc.* **1992**, *114*, 8307.
(33) Hu, J. Z.; Alderman, D. W.; Chaohui, Y.; Pugmire, R. J.; Grant, D. M. *J. Magn. Reson. A* **1993**, *105*, 82−87.
(34) Lipmaa, E.; Alla, M.; Turherm, T. In *Proceedings of the XIXth Congress Ampere*; Heidelberg, 1976; p 241.
(35) Yarim-Agaev, Y.; Tutunjian, P. N.; Waugh, J. S. *J. Magn. Reson.* **1982**, *47*, 51−60.
(36) Bax, A.; Szeverenyi, N. M.; Maciel, G. E. *J. Magn. Reson.* **1983**, *51*, 400−408.
(37) Tycko, R.; Dabbagh, G.; Mirau, P. A. *J. Magn. Reson.* **1989**, *85*, 265−274.
(38) Bax, A.; Szeverenyi, N. M.; Maciel, G. E. *J. Magn. Reson.* **1983**, *55*, 494−497.
(39) Nakai, T.; Ashida, J.; Terao, T. *J. Chem. Phys.* **1988**, *88*, 6049−6058.
(40) Frydman, L.; Chingas, G. C.; Lee, Y. K.; Grandinetti, P. J.; Eastman, M. A.; Barrall, G. A.; Pines, A. *J. Chem. Phys.* **1992**, *97*, 4800−4808.
(41) Chaturvedi, S.; Kuantee, G.; Parthasarathy, R. *Biopolymers* **1991**, *31*, 397−407.
(42) Fawcett, J. K.; Camerman, N.; Camerman, A. *Acta Crystallogr. B* **1975**, *31*, 658−665.
(43) Hempel, A.; Camerman, N.; Camerman, A. *Biopolymers* **1991**, *31*, 187−192.
(44) Ten Kortenaar, P. B. W.; Van Dijk, B. G.; Peeters, J. M.; Raaben, B. J.; Adam, P. J. H. M.; Tesser, G. I. *Int. J. Peptide Protein Res.* **1986**, *27*, 398−400.

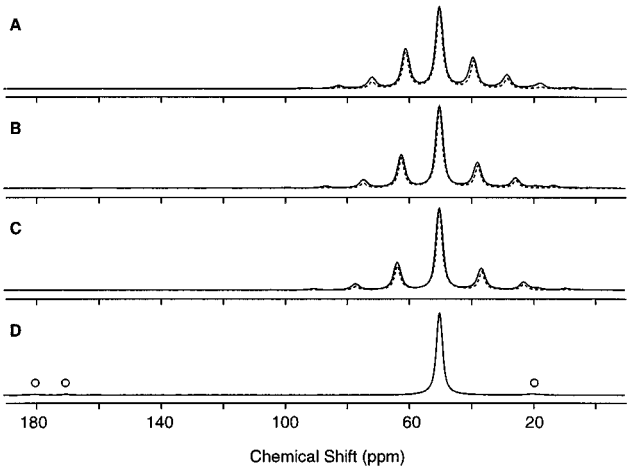

Figure 1. CPMAS spectra for crystalline $^{13}C_\alpha$-labeled A*AA-hemihydrate (solid lines) and their best fits (dashed lines). For all experiments, the CP contact time was 2.5 ms, the decoupling field strength was 108 kHz, and the recycle delay was 1.5 s. **A.** 40 960 scans were acquired, spinning at 821 Hz. **B.** 24 576 scans were acquired, spinning at 928 Hz. **C.** 28 672 scans were acquired, spinning at 1024 Hz. **D.** 2048 scans were acquired, spinning at 10 kHz. This spectrum was not fit, since it contains little information about the CSA. Open circles show natural abundance ^{13}C sites. All chemical shifts are referenced to $^{13}C{=}O$ glycine at 176.04 ppm.

the isotropic shift, δ_{11}, δ_{22}, and the line widths, were simultaneously fit. The simulation using Floquet theory[45−47] was written in the NMR simulation environment GAMMA.[48] Powder averages were perfomed using the method of Cheng et al.[49] to obtain an optimal coverage of the sphere. The presence of the directly attached ^{14}N introduced both a dipolar and a quadrupolar contribution to the sideband pattern. The quadrupolar interaction has been previously determined to be negligible[50−53] (less than 20 Hz at 75 MHz) and was therefore not included. However, the $^{14}N-^{13}C$ dipolar coupling is comparible in magnitude to, but smaller than, the $^{13}C_\alpha$ CSA. This interaction has been analyzed in detail for the carbonyl carbon[54] and can be extended to the C_α by using an additional rotation to bring the CSA into the dipolar frame. Following Tycko,[54] a "local-field tensor", $\vec{\delta}^*(\mu)$, can be defined, such that $\vec{\delta}^*(\mu) = \vec{\delta} + \vec{D}(m)$ where $\vec{D}(m)$ is the dipolar correction to $\vec{\delta}$, the chemical shift tensor. Thus, $\vec{\delta}$ is brought into the dipolar frame by rotating around two Euler angles, α and β, where α represents a rotation around δ_{33} and β represents a subsequent rotation around δ_{22}'. Adding $\vec{D}(m)$ and diaganolizing the resultant tensor, the effective CSA for each of the three ^{14}N spin states can be calculated. The observed MAS spectrum is the superposition of the subspectra due to these three local-field tensors. MAS subspectra were calculated for each of the ^{14}N spin states using the orientation of the CSA with respect to the $^{14}N-^{13}C$ bond determined in our theoretical calculations for GA*V, ($\alpha = -47.3°$, $\beta = 71.9°$) and a dipolar coupling of 712.7 Hz, corresponding to a $^{14}N-^{13}C$ bond distance of 1.45 Å. The experimental data were fit to the sum of the resulting subspectra, and errors were calculated. An average of the CSA values derived from each of the three experiments was taken and used to compare with theoretically calculated values. Isotropic-shift values were measured relative to the carbonyl carbon of glycine at 176.04 ppm.

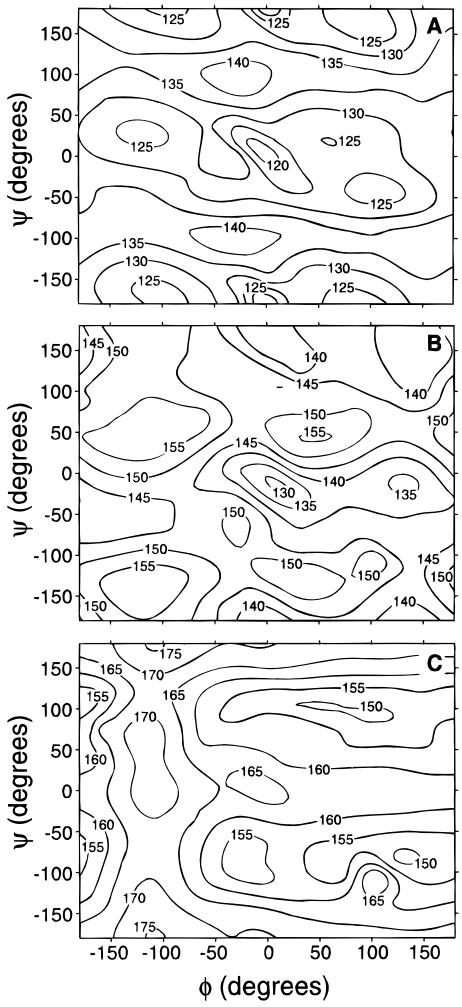

Figure 2. Alanine Ramachandran shielding surfaces for C_α sites in *N*-formyl-L-alanine amide. **A.** σ_{11}; **B.** σ_{22}; **C.** σ_{33}. Surfaces were approximated using 358 points spread over ϕ/ψ space with a more dense placement of points in allowed regions.

Computational

Shielding calculations were performed using the TEXAS-90 program[55] which utilizes the gauge-including-atomic-orbital (GIAO) method.[56,57] All calculations were done on an *N*-formyl-L-alanine amide fragment extensively minimized at the helical geometry. A "locally dense" basis set was employed consisting of 6-311++G(2d,2p) basis functions on the central residue and 6-31G basis functions on the formyl and amide groups. Computations were performed on IBM RISC/6000 workstations (Models 340, 350, and 360; IBM Corporation, Austin, TX). The shielding surfaces were constructed by choosing 358 ϕ,ψ points in Ramachandran space, with a more dense placement of points in the allowed regions. Z-surfaces for the chemical-shift tensors were created using a Gaussian equation

$$Z_{\delta_{nn}}(\phi,\psi) = \exp[-(\delta_{nn}^{ess} - \delta_{nn}(\phi,\psi))^2/\omega^2]$$

(45) Shirley, J. H. *Phys. Rev. B* **1965**, *138*, 979.
(46) Vega, S. *J. Chem. Phys.* **1992**, *96*, 2655−2680.
(47) Levante, T. O.; Baldus, M.; Meier, B. H.; Ernst, R. R. *Mol. Phys.* **1995**, *86*, 1195−1212.
(48) Smith, S. A.; Levante, T. O.; Meier, B. H.; Ernst, R. R. *J. Magn. Reson.* **1994**, *A106*, 75−105.
(49) Cheng, V. B.; Suzukawa, H. H.; Wolfsberg, M. *J. Chem. Phys.* **1973**, *59*, 3992−3999.
(50) Hexem, J. G.; Frey, M. H.; Opella, S. J. *J. Am. Chem. Soc.* **1981**, *103*, 224.
(51) Zumbulyadis, N.; Henrichs, P. M.; Young, R. H. *J. Chem. Phys.* **1981**, *75*, 1603.
(52) Naito, A.; Ganapathy, S.; McDowell, C. A. *J. Chem. Phys.* **1981**, *74*, 5393.
(53) Naito, A.; Ganapathy, S.; McDowell, C. A. *J. Magn. Reson.* **1982**, *48*, 367.
(54) Tycko, R.; Weliky, D. P.; Berger, A. E. *J. Chem. Phys.* **1996**, *105*, 7915−7930.
(55) Wolinski, K.; Hinton, J. F.; Pulay, P. *J. Am. Chem. Soc.* **1990**, *112*, 8251−8260.
(56) London, F. *J. Phys. Radium* **1937**, *8*, 397−409.
(57) Ditchfield, R. *J. Chem. Phys.* **1972**, *56*, 5688−5691.

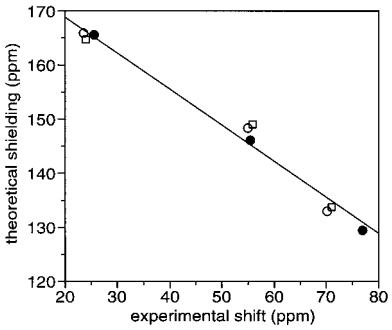

Figure 3. Theoretical $^{13}C_\alpha$ chemical-shift tensor elements for G*AV (filled circles), A*AA (open circles) and A*AA-hemihydrate (open squares) calculated using the GIAO method and dihedral angles taken from the crystal structures versus the experimentally measured tensors (slope = −0.67, *y*-intercept = 182.17, $R = 0.99$, and rmsd = 2.15). For G*AV, the experimentally determined values (in ppm) were $\delta_{11} = 76.9 \pm 0.04$, $\delta_{22} = 55.4 \pm 0.05$, $\delta_{33} = 25.5 \pm 0.09$, and the calculated values were $\sigma_{11} = 129.45$, $\sigma_{22} = 146.18$, and $\sigma_{33} = 164.46$. For A*AA, the experimentally determined values were $\delta_{11} = 70.2 \pm 0.2$, $\delta_{22} = 54.9 \pm 0.2$, $\delta_{33} = 23.6 \pm 0.4$, and the calculated values were $\sigma_{11} = 132.93$, $\sigma_{22} = 148.20$, and $\sigma_{33} = 165.92$. For A*AA-hemihydrate, the experimentally determined values were $\delta_{11} = 71.0 \pm 1.2$, $\delta_{22} = 55.8 \pm 1.6$, $\delta_{33} = 24.0 \pm 2.8$, and the calculated values were $\sigma_{11} = 133.75$, $\sigma_{22} = 148.95$, and $\sigma_{33} = 164.65$.

where δ_{nn}^{ess} is the experimental chemical-shift tensor, $\delta_{nn}(\phi,\psi)$ is the chemical-shift tensor surface, and ω is the root-mean-square deviation for the theory/experiment correlation. All surfaces were approximated using a Matlab (The Mathworks, Boston, MA) "best fit" function.

Results and Discussion

The CPMAS spectra of crystalline $^{13}C_\alpha$-labeled A*AA-hemihydrate at spinning speeds of 821, 928, 1024, and 10 kHz are shown in Figure 1. Similar data were collected for crystalline $^{13}C_\alpha$-labeled G*AV and for the other A*AA crystal form (data not shown). Although two molecules with slightly different conformations exist in the unit cells of both forms of A*AA, the resolution of our experiments was not high enough to differentiate between them, and only one line was observed. Isotropic shifts were determined for each tripeptide using the fast spinning spectrum referenced to the carbonyl carbon of glycine at 176.04 ppm. For each slow spinning spectrum, nonlinear least-square fits were used to determine the chemical-shift tensor (Figure 1) and error estimates. The average value of the three measurements was used. These were (in ppm) as follows: A*AA: $\delta_{11} = 70.2 \pm 0.2$, $\delta_{22} = 54.9 \pm 0.2$, $\delta_{33} = 23.6 \pm 0.4$; A*AA-hemihydrate: $\delta_{11} = 71.0 \pm 1.2$, $\delta_{22} = 55.8 \pm 1.6$, $\delta_{33} = 24.0 \pm 2.8$; G*AV: $\delta_{11} = 76.9 \pm 0.04$, $\delta_{22} = 55.4 \pm 0.05$, $\delta_{33} = 25.5 \pm 0.09$.

In Figure 2, we show the computed alanine chemical-shielding surfaces for σ_{11} (A), σ_{22} (B), and σ_{33} (C). Using these surfaces and backbone dihedral angles from the X-ray studies, theoretical chemical-shielding values for each of the tripeptides were calculated and compared with the experimental values found above (Figure 3). Two correlations were calculated, one for the three tripeptides G*AV, A*AA, and A*AA-hemihydrate and one for only A*AA and A*AA-hemihydrate. Although the slopes of the best fit lines (−0.67 for G*AV, A*AA, and A*AA-hemihydrate, and −0.66 for A*AA and A*AA-hemihydrate) are not unity, correlation coefficients of $R = 0.99$ and $R = 0.98$ and rmsd values of $\omega = 2.15$ and $\omega = 2.58$ ppm were observed. The low rmsd values demonstrate that the backbone dihedral angles are the main determinants of the tensor components of the C_α chemical shift. To determine if the correlation is unique, i.e., to determine if the tensor components alone are sufficient to predict ϕ and ψ, the Z-surface method[28] was used.

For a given observable, such as a component of the CSA tensor, it is possible to define a surface in ϕ/ψ space which gives the Bayesian probability that the observed value corresponds to a particular ϕ/ψ pair. In the case of a Z-surface, this probability is defined by the Gaussian function given above. As one can see from the Z-surface in Figure 4A, a single parameter, i.e., the C_α isotropic shift, is insufficient to determine uniquely two independent variables (such as two backbone angles), but three parameters are usually sufficient. This was

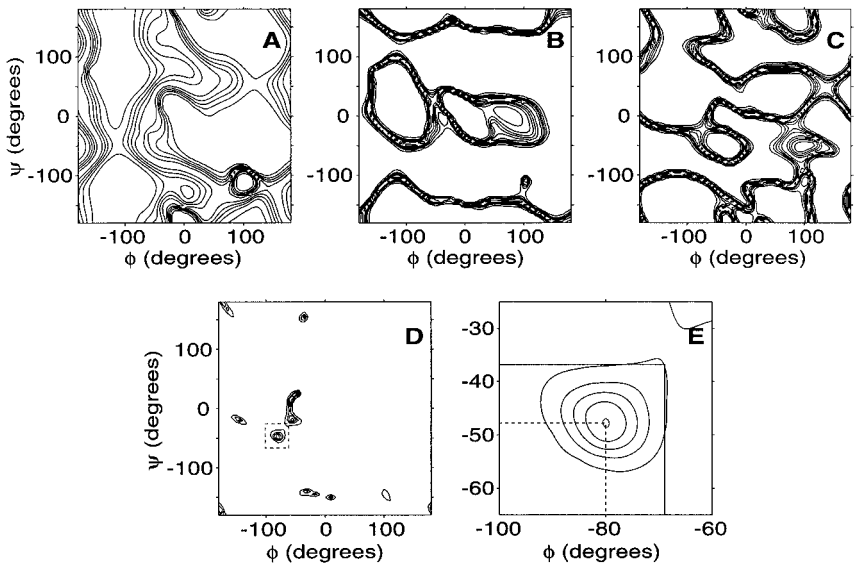

Figure 4. Z-surfaces calculated from the experimentally determined chemical-shift anisotropy for the C_α alanine in G*AV and theoretical chemical-shielding surfaces scaled by the correlation determined using A*AA and A*AA-hemihydrate. **A.** ^{1}Z-surface for the isotropic shift. **B.** ^{1}Z-surface for the width of the CSA ($\delta_{33}-\delta_{11}$). **C.** ^{1}Z-surface for the breadth of the CSA ($\delta_{22}-\delta_{11}$). **D.** ^{3}Z-surface showing the intersection of the surfaces from A, B, and C. The boxed region contains the area of highest probability and is expanded in **E.** The dihedral angles as determined by measurement of the CSA tensor are $\phi = -79.9°$, $\psi = -47.8°$ (dashed lines), while those determined in the crystal structure are $\phi = -68.7°$, $\psi = -38.1°$ (solid lines). These ^{1}Z-surfaces were calculated using an rmsd, $\omega = 2.58$ ppm. In all cases, contours are plotted at 10%, 30%, 50%, 70%, and 90% of the maximum intensity.

demonstrated in solution studies in which the isotropic shifts of the C_α, C_β, and H_α were measured and used to calculate Z-surfaces for the backbone angles, and the intersection of these three Z-surfaces generally narrowed the solution to a single ϕ/ψ pair.[28]

In solids, additional experiments to determine the C_β and H_α isotropic shifts are not needed, since the three components of the chemical-shift anisotropy, δ_{11}, δ_{22}, and δ_{33}, provide the necessary three independent parameters. Because the isotropic-shift value is contained in δ_{11}, δ_{22}, and δ_{33}, even small errors in its measurement would be amplified in a product of those three Z-surfaces. Three alternative parameters, the isotropic shift, the width of the CSA ($\delta_{33}-\delta_{11}$) and the breadth of the CSA ($\delta_{22}-\delta_{11}$) were used to eliminate the propagation of error. The ^{1}Z width, breadth, and isotropic surfaces for G*AV are shown in Figure 4 along with the ^{3}Z surface which represents the product of the three ^{1}Z surfaces. When the correlation based only on A*AA and A*AA-hemihydrate data is used to scale the calculated tensor surfaces, three high-probability solutions are predicted (Figures 4D-E) for G*AV. The highest probability solution (Gaussian probability, $P = 0.91$) is $\phi = -79.9°$ and $\psi = -47.8°$, which is close to the values determined by X-ray crystallography ($\phi = -68.7°$ and $\psi = -38.1°$). Of the other two high probability solutions, one ($P = 0.84$) is in an allowed region ($\phi = -55.8°$, $\psi = -18.8°$), while the other ($P = 0.82$) is sterically unallowed ($\phi = -59.5°$, $\psi = 10.1°$).

Although there are two possible solutions in the allowed regions of Ramachandran space, we expect that the accuracy of predictions will increase as more data points are used to calculate the correlation of theory and experiment, and as experiments are carried out at higher field where the ratio of the CSA to the dipolar coupling is larger. However, several factors could lead to a decrease in accuracy. In general the effects of motion on the CSA must be accounted for, although these effects could be ignored in our study since crystalline peptides were used. Deuterium relaxation studies might be used to determine the effects of motion when necessary, however this might introduce larger uncertainties. Lower signal-to-noise or overlapping spectra would also lead to a decrease in the accuracy of dihedral angle predictions. Our results nevertheless demonstrate that the three tensor components are sufficient to greatly narrow the possible ϕ/ψ angles and to allow accurate predictions in the general case.

Conclusions

We have described a simple method for the determination of dihedral angles in peptides and proteins in the solid state. We have measured the chemical-shift tensors of the central $^{13}C_\alpha$ in three crystalline tripeptides by slow CPMAS, and have correlated the measured values with shieldings calculated by *ab initio* methods. This correlation was then used to calculate ϕ/ψ Z-surfaces for the three components of the CSA, and the intersection of the three surfaces predicted ϕ/ψ pairs. For G*AV, three high probability ϕ/ψ pairs were predicted. The highest probability pair lies within $\pm 12°$ of the ϕ/ψ pair determined in the crystal structure. The results demonstrate that the tensor components of a single site are sufficient to greatly narrow the possible dihedral angles and, in the best case, to accurately predict them. Furthermore, the inclusion of Z-surfaces for C_β and C_γ chemical-shift tensors as well as Z-surfaces which predict the orientation of the CSA should provide additional constraints on the backbone dihedral angles as well as provide constraints on side-chain torsion angles, thereby increasing the predictive power of the CSA/Z surface method.

Acknowledgment. The authors thank Andrea Sefler and Bruce Ellsworth for synthesis help and Jaru Jancarik for help with crystallization. J.H. and D.D.L gratefully acknowledge the Howard Hughes Medical Institute for predoctoral fellowships. M.T. acknowledges support from the Swiss National Foundation of Science. R.H.H. is a Barry Goldwater Fellow. D.E.W. would like to thank the Keck Foundation for providing support for computing. The research in Berkeley was funded by the Director, Office of Energy Research, Office of Basic Energy Sciences, Materials Sciences Division, U.S. Department of Energy, under Contract No. DE-AC03-76SF0098 and by NIH Grant AG10770. The research in Illinois was supported in part by the United States Public Health Service (NIH Grant Nos. HL-19481 and GM-50694).

JA970124K